2-(Thienyl)quinoxaline derivatives and their application in Ir(III) complexes as tuneable deep red emitters

Sophie A. Fitzgerald, Ellie N. Payce, Peter N. Horton,

Simon J. Coles and Simon J.A. Pope*

Electronic Supplementary Information (ESI)

Contents

Experimental: Synthesis of ligand precursors and previously reported ligands, L^1H, L^6H, $L^{10}H$ and $L^{11}H$

Synthesis of 2-bromo-1-(thiophen-2-yl)ethan-1-one

A simple bromination reaction took place, where dioxane dibromide (1.10 g, 8.05mmol) in a solution of 1,4-dioxane and diethyl ether (1:1, 40 mL) was added dropwise to 2-acetyl thiophene (0.92 g, 7.31 mmol) in the same solvent mixture over 2 h whilst stirring under air at room temperature. The solution was added to water and extracted with diethyl ether. The combined organic layers were dried over $MgSO_4$, and the solvent was removed *in vacuo* to yield a brown/yellow oil (1.49 g, 99%). ^{1}H NMR (400 MHz, $CDCl_3$) δ_H = 7.80 (dd, $^3J_{HH}$ = 3.8, $^4J_{HH}$ = 1.1 Hz, 1H), 7.71 (dd, $^3J_{HH}$ = 5.0, $^4J_{HH}$ = 1.1 Hz, 1H), 7.16 (dd, $^3J_{HH}$ = 4.9, 3.9 Hz, 1H), 4.36 (s, 2H) ppm. The data is consistent with literature values.[1]

Synthesis of 2-bromo-1-(5-bromothiophen-2-yl)ethan-1-one

Prepared similarly from 2-acetyl-5-bromothiophene (1.08 g, 5.28 mmol) and dioxane dibromide (1.43 g, 5.81 mmol) to give the product as an off white solid (1.39 g, 93%). ^{1}H NMR (400 MHz, $CDCl_3$) δ_H = 7.55 (d, $^3J_{HH}$ = 4.1 Hz, 1H), 7.14 (d, $^3J_{HH}$ = 4.1 Hz, 1H), 4.28 (s, 2H) ppm.

Synthesis of 2-bromo-1-(5-chlorothiophen-2-yl)ethan-1-one

Prepared similarly from 2-acetyl-5-chlorothiophene (1.01 g, 6.26 mmol) and dioxane dibromide (1.71 g, 6.89 mmol) to give the product as an off white solid (1.06 g, 71%). ^{1}H NMR (400 MHz, $CDCl_3$): δ_H = 7.60 (d, $^3J_{HH}$ = 4.1 Hz, 1H), 7.00 (d, $^3J_{HH}$ = 4.1 Hz, 1H), 4.28 (s, 2H) ppm.

Synthesis of 2-bromo-1-(5-iodothiophen-2-yl)ethan-1-one

A modified bromination method was adopted, where 2-acetyl-5-iodothiophene (1.00 g, 3.97 mmol) was dissolved in glacial acetic acid (15 mL) and dioxane dibromide (0.984 g, 3.97 mmol) in acetic acid (6 mL) was added dropwise. The mixture was stirred at room temperature under an inert nitrogen atmosphere in the absence of light for 24 h. The solvent

was removed *in vacuo*, ensuring that the temperature remained under 40°C. The residue was dissolved in dichloromethane and washed with saturated aqueous $NaHCO_3$, water and saturated aqueous NaCl. The combined organic layers were dried over $MgSO_4$, then the solvent was removed *in vacuo* to give the product as a brown solid (1.23 g, 93 %). ^{1}H NMR (500 MHz, $CDCl_3$): δ_H = 7.42 (d, $^3J_{HH}$ = 4.0 Hz, 1H), 7.34 (d, $^3J_{HH}$ = 4.0 Hz, 1H), 4.28 (s, 2H) ppm. $^{13}C\{^1H\}$ NMR (126 MHz, $CDCl_3$) δ_C = 183.1, 146.6, 138.5, 134.4, 87.4, 30.2 ppm. HRMS (EI): found *m/z* 329.8209, calc'd *m/z* 329.8211 for $C_6H_4OSBr^{127}I$. FTIR (solid, ATR) ν_{max} / cm^{-1}: 3084, 3073, 2996, 2949, 1663, 1638, 1510, 1396, 1389, 1312, 1271, 1215, 1192, 1146, 1067, 1034, 1015, 959, 924, 903, 870, 795, 762, 739, 679, 662, 638, 603, 596, 573, 540, 474, 444, 415.

Synthesis of 1-([2,2'-bithiophen]-5-yl)-2-bromoethan-1-one

Prepared similarly to 2-bromo-1-(thiophen-2-yl)ethan-1-one from 5-acetyl-2,2'-bithienyl (122 mg, 0.585 mmol) and dioxane dibromide (174 mg, 0.702 mmol) to give the crude product. The pure product was obtained by column chromatography (SiO_2) where the band eluted at 99:1 CH_2Cl_2:CH_3OH to give the product as a dark yellow solid (118 mg, 70%). ^{1}H NMR (400 MHz, $CDCl_3$) δ_H = 7.70 (d, $^3J_{HH}$ = 4.0 Hz, 1H), 7.37 – 7.34 (m, 2H), 7.20 (d, $^3J_{HH}$ = 4.0 Hz, 1H), 7.07 (dd, $^3J_{HH}$ = 5.0, 3.7 Hz, 1H), 4.34 (s, 2H) ppm. $^{13}C\{^1H\}$ NMR (101 MHz, $CDCl_3$) δ_C = 184.2, 147.5, 138.6, 136.1, 134.6, 128.5, 127.2, 126.3, 124.5, 30.2 ppm. HRMS (CI): found *m/z* 285.9115, calc'd *m/z* 285.91162 for $C_{10}H_7O^{79}Br^{32}S_2$. FTIR (solid, ATR) ν_{max} / cm^{-1}: 3084, 3034, 2922, 2853, 1665, 1639, 1504, 1443, 1422, 1358, 1310, 1273, 1204, 1192, 1159, 1115, 1065, 1051, 1034, 972, 934, 887, 839, 799, 750, 741, 702, 640, 610, 592, 542, 488, 446.

Synthesis of 2-bromo-1-(thiophen-3-yl)ethan-1-one[2]

The brominated compound was prepared *via* a modified synthetic method. 3-Acetylthiophene (804 mg, 6.372 mmol) in a solution of 1,4-dioxane and diethyl ether (1:1, 40 mL) was heated to 70°C under an inert nitrogen atmosphere whilst stirring. Dioxane dibromide (1.730 g, 7.010 mmol) in the same solvent mixture (40 mL) was added dropwise over 2 h. The reaction mixture was heated to reflux for a further 24 h. The mixture was monitored by thin-layer chromatography (DCM, SiO_2). Upon cooling to room temperature, the mixture was washed with distilled water (30 mL) and extracted with diethyl ether (3 × 25 mL). The combined organic layers were dried over $MgSO_4$ and the solvent was removed

in vacuo giving rise to the crude product. Purification took place by column chromatography (DCM → DCM:MeOH, 9:1) where the pure product was obtained as an off-white crystalline solid (752 mg, 58%). ^{1}H NMR (400 MHz, $CDCl_3$) δ_H = 8.18 (dd, $^{4}J_{HH}$ = 2.9, 1.3 Hz, 1H), 7.58 (dd, $^{3}J_{HH}$ = = 5.1, $^{4}J_{HH}$ = 1.3 Hz, 1H), 7.36 (dd, $^{3}J_{HH}$ = 5.1, $^{4}J_{HH}$ = 2.9 Hz, 1H), 4.34 (s, 2H) ppm. $^{13}C\{^{1}H\}$ NMR (101 MHz, $CDCl_3$) δ_C = 185.7, 138.9, 133.9, 127.4, 127.0, 31.7 ppm.

Synthesis of 2-(thiophen-2-yl)quinoxaline (L^1H)[3]

2-bromo-1-(thiophen-2-yl)ethan-1-one (1.49 g, 7.26 mmol) and 1,2-phenylenediamine (0.86 g, 7.99 mmol) were heated to reflux in ethanol (10mL) for 24 h under an inert nitrogen atmosphere. The formation of a precipitate took place upon cooling the mixture to room temperature, and the resultant suspension was filtered under reduced pressure. This was washed with a small amount of cold ethanol to give the product as an orange solid (0.33 g, 22%). ^{1}H NMR (400 MHz, $CDCl_3$) δ_H = 9.24 (s, 1H), 8.09 – 8.04 (m, 2H), 7.86 (dd, $^{3}J_{HH}$ = 3.7, $^{4}J_{HH}$ = 1.1 Hz, 1H), 7.77 – 7.67 (m, 2H), 7.55 (dd, $^{3}J_{HH}$ = 5.0, $^{4}J_{HH}$ = 1.1 Hz, 1H), 7.21 (dd, $^{3}J_{HH}$ = 5.0, 3.7 Hz, 1H) ppm. $^{13}C\{^{1}H\}$ NMR (101 MHz, $CDCl_3$) δ_C = 147.5, 142.4, 142.3, 142.2, 141.5, 130.6, 130.0, 129.4, 129.3, 129.3, 128.6, 127.1 ppm. HRMS (EI): found *m/z* 212.0411, calc'd *m/z* 212.0408 for $C_{12}H_8N_2S$. UV-vis (MeCN) λ_{max} ($\varepsilon \times 10^4$ / L mol^{-1} cm^{-1}): 217 (3.2), 272 (2.1), 353 (1.6), 368 (1.5) nm. FTIR (solid, ATR) ν_{max} / cm^{-1}: 3121, 3059, 2363, 2330, 1734, 1545, 1491, 1427, 1319, 1238, 1207, 1134, 1125, 1074, 1053, 997, 941, 926, 866, 851, 758, 721, 677, 613, 583, 567, 542, 471, 419, 407.

Synthesis of 6,7-dimethyl-2-(thiophen-2-yl)quinoxaline (L^6H)[4]

Prepared similarly from 2-bromo-1-(thiophen-2-yl)ethan-1-one (500 mg, 2.44 mmol) and 4,5-dimethyl-*o*-phenylenediamine (365 mg, 2.68 mmol) to give the product as a yellow solid (270 mg, 46%). ^{1}H NMR (400 MHz, $CDCl_3$) δ_H = 9.14 (s, 1H), 7.83 (s, 1H), 7.81 (dd, $^{3}J_{HH}$ = 3.7, $^{4}J_{HH}$ = 1.0 Hz, 1H), 7.79 (s, 1H), 7.51 (dd, $^{3}J_{HH}$ = 5.0, $^{4}J_{HH}$ = 1.0 Hz, 1H), 7.19 (dd, $^{3}J_{HH}$ = 5.0, 3.7 Hz, 1H), 2.48 (s, 6H) ppm. $^{13}C\{^{1}H\}$ NMR (101 MHz, $CDCl_3$) δ_C = 146.7, 142.8, 141.2, 141.1, 141.2, 140.4, 139.9, 129.3, 128.5, 128.3, 126.4, 20.5, 20.4 ppm. UV-vis (CH_3CN): λ_{max} ($\varepsilon \times 10^4$ / L mol^{-1} cm^{-1}): 222 (3.5), 273 (2.4), 357 (2.1), 373 (2.1) nm. FTIR (solid, ATR) ν_{max} / cm^{-1}: 3069, 3034, 1541, 1487, 1422, 1317, 1213, 1082, 1067, 1024, 1005, 930, 872, 847, 704, 638, 621, 494, 428.

Synthesis of 2,3-di(thiophen-2-yl)quinoxaline ($L^{10}H$)[5]

2,2'-thenil (100 mg, 0.450 mmol) and 1,2-phenylenediamine (54 mg, 0.495 mmol) were dissolved in ethanol (15 mL). A catalytic amount of acetic acid (0.5 mL) was added and the reaction mixture was heated to reflux and stirred for 24 h under an inert nitrogen atmosphere. Upon cooling to room temperature, the solvent was removed *in vacuo*, and the crude product was dissolved in dichloromethane and washed with 0.1M HCl (2 x 10 mL). The organic layer was dried over $MgSO_4$ and the solvent was removed *in vacuo* to give the product as a pale yellow crystalline solid (125 mg, 95 %). ^{1}H NMR (400 MHz, $CDCl_3$) δ_H = 8.08 (dd, $^3J_{HH}$ = 6.3, $^4J_{HH}$ = 3.5 Hz, 1H), 7.72 (dd, $^3J_{HH}$ = 6.4, $^4J_{HH}$ = 3.4 Hz, 1H), 7.50 (dd, $^3J_{HH}$ = 5.0, $^4J_{HH}$ = 0.8 Hz, 1H), 7.26 (d, $^3J_{HH}$ = 3.7 Hz, 1H), 7.05 (dd, $^3J_{HH}$ = 4.8, 3.9 Hz, 1H) ppm. UV-vis (MeCN) λ_{max} ($\varepsilon \times 10^4$ / L mol^{-1} cm^{-1}): 208 (2.3), 252 (1.8), 286 (1.4), 378 (1.0) nm.

Synthesis of 2-(thiophen-3-yl)quinoxaline ($L^{11}H$)[6]

The ligand was prepared similarly to **L^1H** with slight modifications, where 2-bromo-1-(thiophen-3-yl)ethan-1-one (728 mg, 3.55 mmol) and 1,2-phenylenediamine (406 mg, 3.76 mmol) were dissolved in ethanol (40 mL) and heated to reflux under an inert nitrogen atmosphere for 24 h. The mixture was cooled to room temperature and the crude product was extracted with CH_2Cl_2 (3 x 20 mL) and washed with distilled water (30 mL). The combined organic layers were dried over $MgSO_4$ and the solvent was removed *in vacuo*. Purification took place using column chromatography ($CH_2Cl_2 \rightarrow CH_2Cl_2$:$CH_3OH$ 9:1, SiO_2) to obtain the pure product as a dark brown solid (619 mg, 82%). ^{1}H NMR (400 MHz, $CDCl_3$) δ_H 9.24 (s, 1H), 8.16 (dd, $^4J_{HH}$ = 2.9, 1.3 Hz, 1H), 8.09 (ddd, $^3J_{HH}$ = 5.8, 5.4, $^4J_{HH}$ = 1.6 Hz, 2H), 7.92 (dd, $^3J_{HH}$ = 5.1, $^4J_{HH}$ = 1.3 Hz, 1H), 7.69-7.80 (m, 2H), 7.50 (dd, $^3J_{HH}$ = 5.1, $^4J_{HH}$ = 2.9 Hz, 1H) ppm. ^{13}C{^{1}H} NMR (126 MHz, $CDCl_3$) δ_C = 148.0, 143.3, 142.3, 141.3, 139.5, 130.4, 129.4, 129.3, 129.1, 127.2, 126.5, 126.0 ppm. UV-vis (MeCN) λ_{max} ($\varepsilon \times 10^4$ / L mol^{-1} cm^{-1}): 213 (2.4), 237 (1.4), 267 (2.4), 339 (1.2), 351 (1.0) nm.

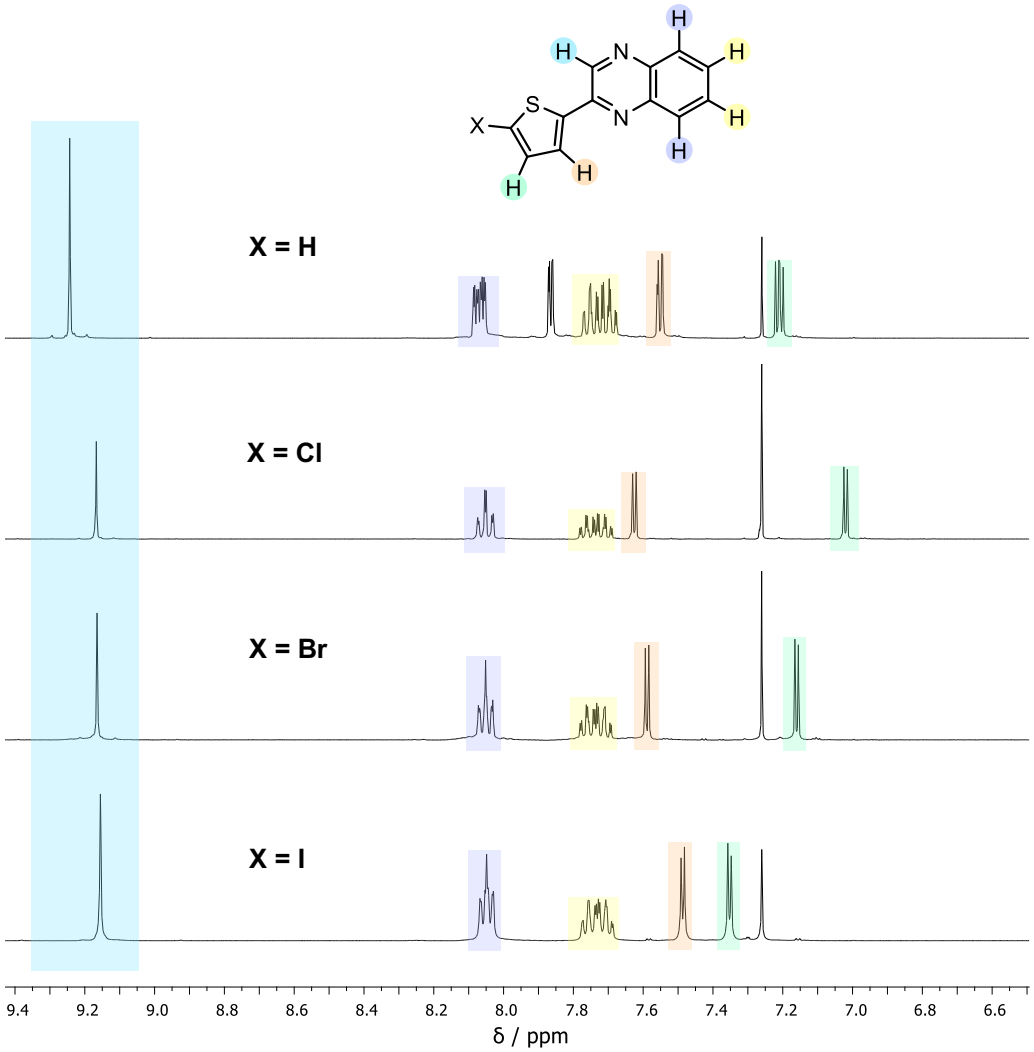

Figure S1. Stacked ^{1}H NMR spectra of **L$^{1\text{-}4}$H**, (400 MHz, $CDCl_3$).

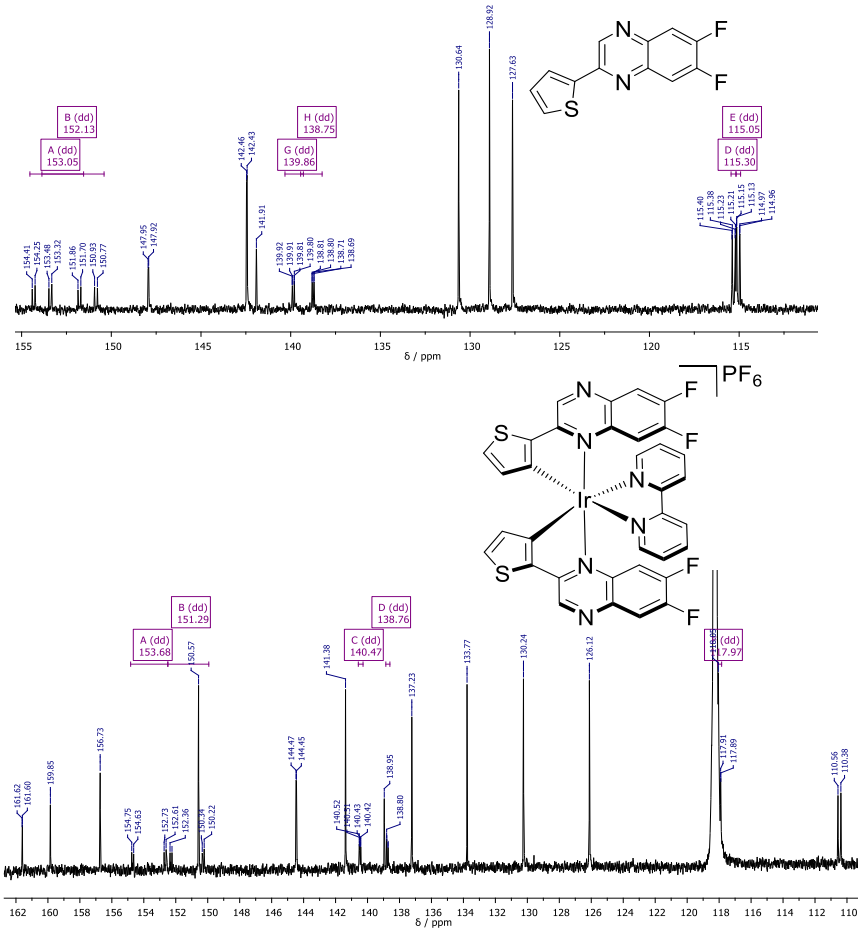

Figure S2. Comparison $^{13}C\{^{1}H\}$ NMR spectra of **L^{7}H** (top) and [Ir(**L^{7}**)$_2$(bipy)]PF$_6$ (101 MHz, $CDCl_3$).

Table S1. Selected peak positions and coupling constants from the $^{13}C\{^{1}H\}$ NMR spectra of **L^{7}H** and [Ir(**L^{7}**)$_2$(bipy)]PF$_6$.

Assignment	δ_C / ppm	
	L^{7}H ($CDCl_3$, 101 MHz)	[Ir(**L^{7}**)$_2$(bipy)]PF$_6$ (CD_3CN, 126 MHz)
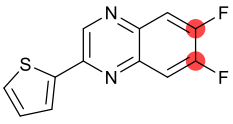	152.9 $^{1}J_{CF}$ = 256.6 Hz, $^{2}J_{CF}$ = 16.1 Hz	153.7 $^{1}J_{CF}$ = 255.0 Hz, $^{2}J_{CF}$ = 15.4 Hz
	151.9 $^{1}J_{CF}$ = 256.0 Hz, $^{2}J_{CF}$ = 16.0 Hz	151.3 $^{1}J_{CF}$ = 253.4 Hz, $^{2}J_{CF}$ = 15.4 Hz
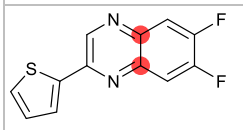	139.7 $^{3}J_{CF}$ = 11.1 Hz, $^{4}J_{CF}$ = 1.2 Hz	140.5 $^{2}J_{CF}$ = 10.4 Hz, $^{3}J_{CF}$ = 1.2 Hz
	138.6 $^{3}J_{CF}$ = 10.6 Hz, $^{4}J_{CF}$ = 1.1 Hz	138.8 $^{2}J_{CF}$ = 10.5 Hz, $^{3}J_{CF}$ = 1.4 Hz
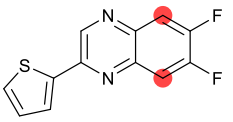	115.1 $^{2}J_{CF}$ = 17.5 Hz, $^{3}J_{CF}$ = 1.9 Hz	118.0 $^{2}J_{CF}$ = 17.9 Hz, $^{3}J_{CF}$ = 2.1 Hz
	114.9 $^{2}J_{CF}$ = 17.5 Hz, $^{3}J_{CF}$ = 1.6 Hz	

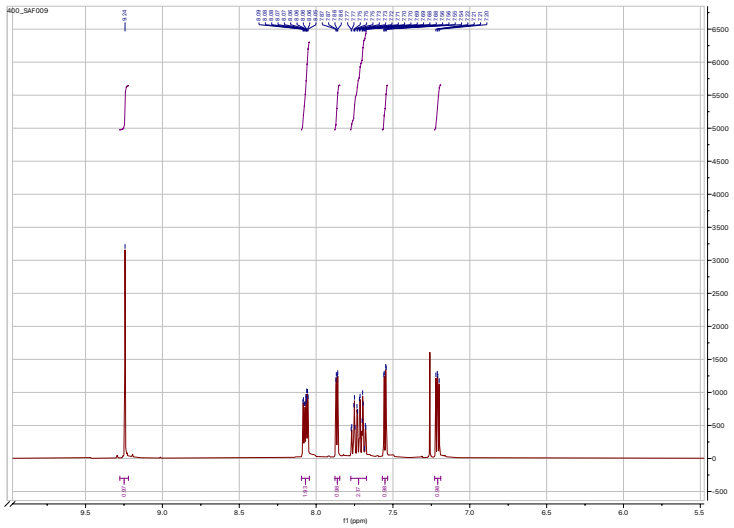

Figure S3. ^{1}H NMR spectrum of L^{1}H.

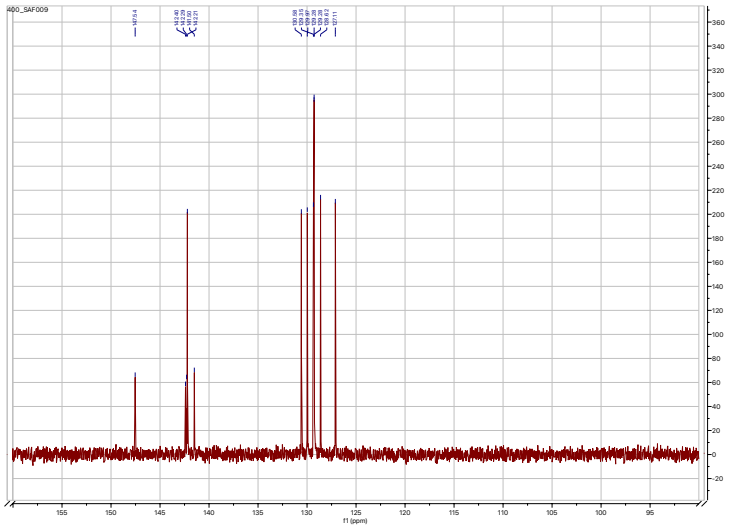

Figure S4. ^{13}C{^{1}H} NMR spectrum of L^{1}H.

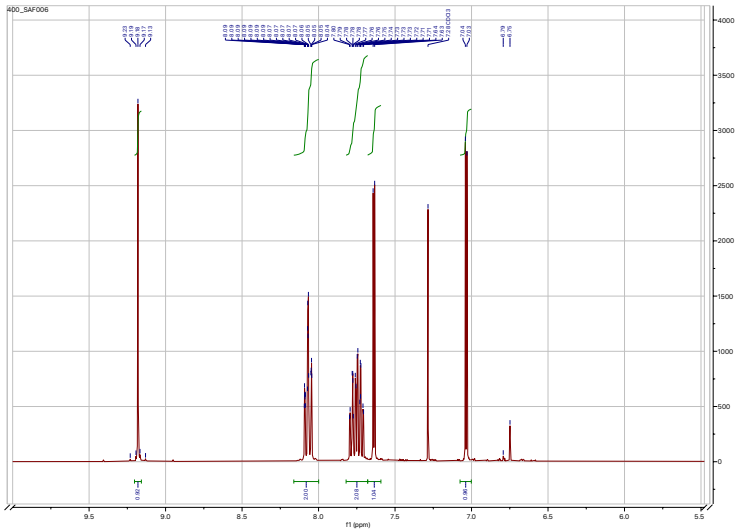

Figure S5. ^{1}H NMR spectrum of L^{2}H.

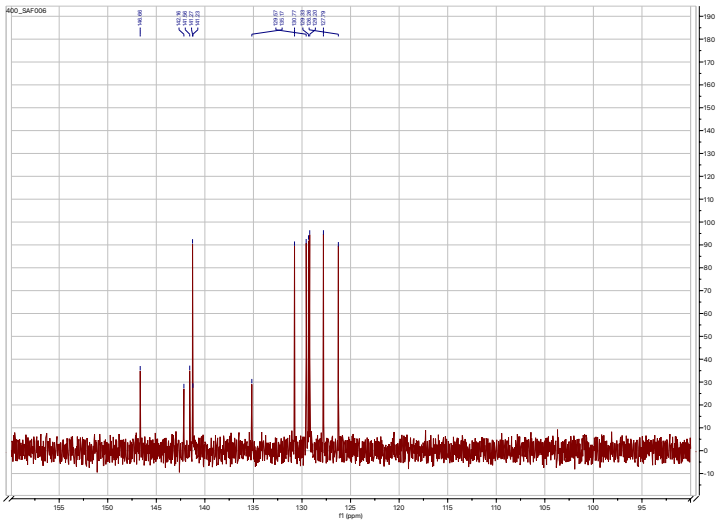

Figure S6. $^{13}C\{^{1}H\}$ NMR spectrum of $L^{2}H$ ($CDCl_3$).

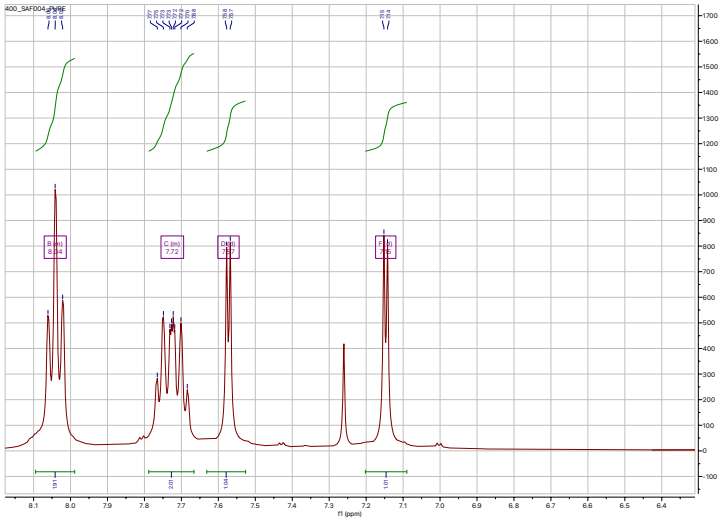

Figure S7. ^{1}H NMR spectrum of $L^{3}H$ ($CDCl_3$).

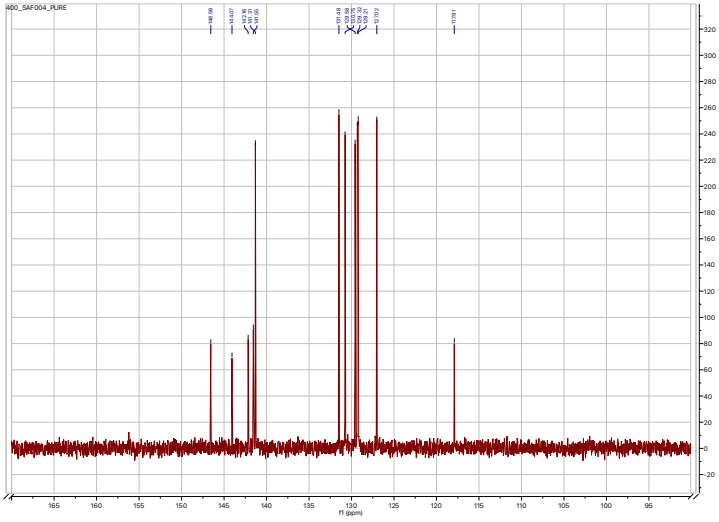

Figure S8. $^{13}C\{^{1}H\}$ NMR spectrum of $L^{3}H$ ($CDCl_3$).

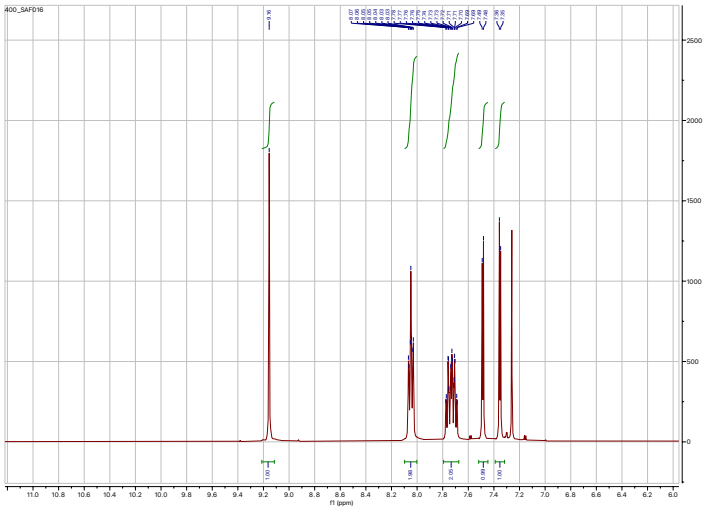

Figure S9. ^{1}H NMR spectrum of $L^{4}H$ ($CDCl_3$).

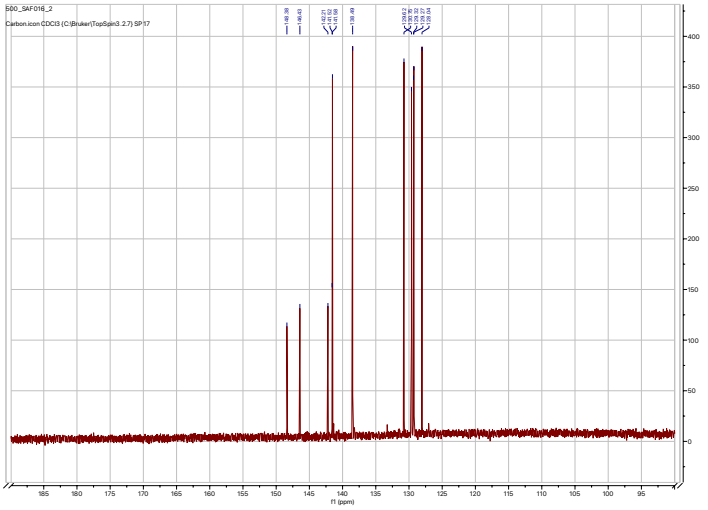

Figure S10. $^{13}C\{^{1}H\}$ NMR spectrum of $L^{4}H$ ($CDCl_3$).

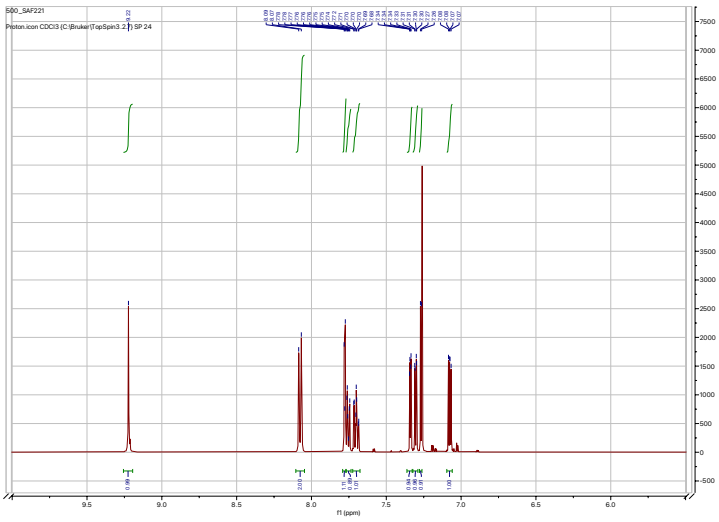

Figure S11. ^{1}H NMR spectrum of $L^{5}H$ ($CDCl_3$).

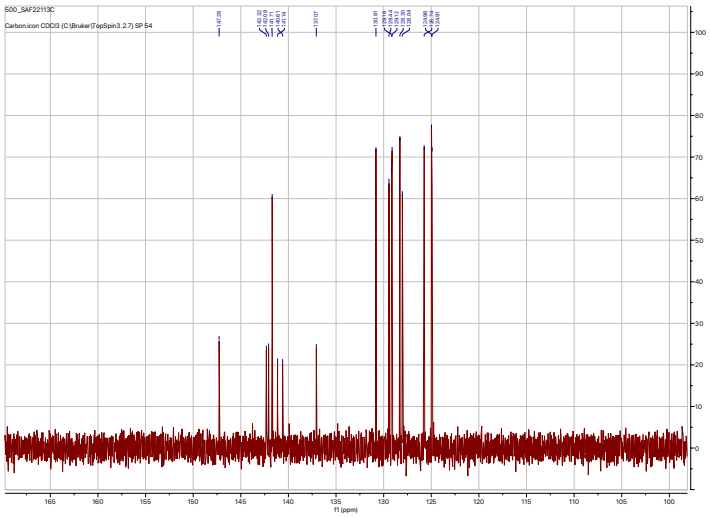

Figure S12. $^{13}C\{^{1}H\}$ NMR spectrum of L^5H ($CDCl_3$).

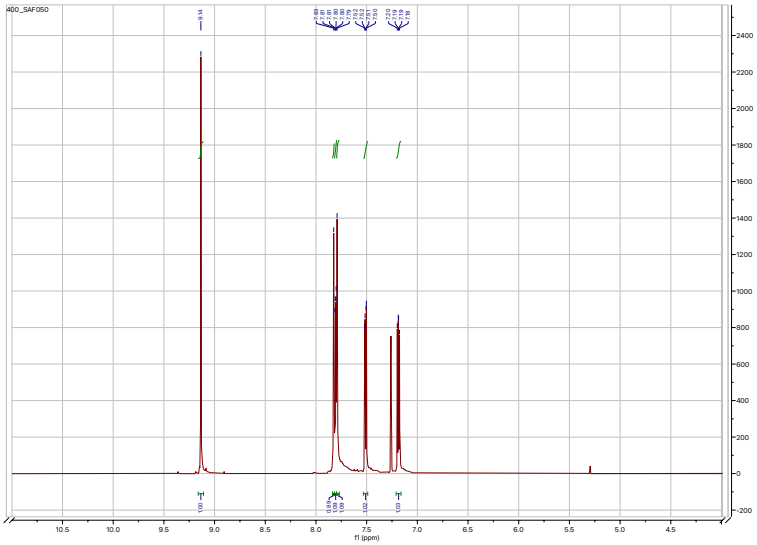

Figure S13. ^{1}H NMR spectrum of L^6H ($CDCl_3$).

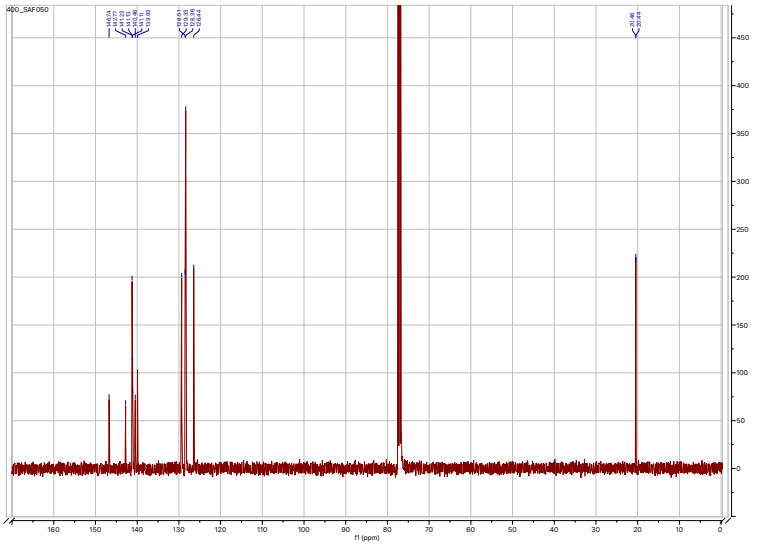

Figure S14. $^{13}C\{^{1}H\}$ NMR spectrum of L^6H ($CDCl_3$).

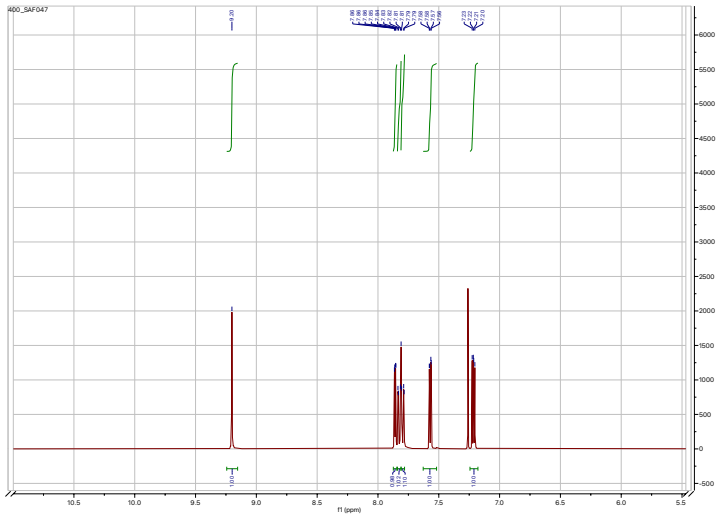

Figure S15. ^{1}H NMR spectrum of $L^{7}H$ ($CDCl_3$).

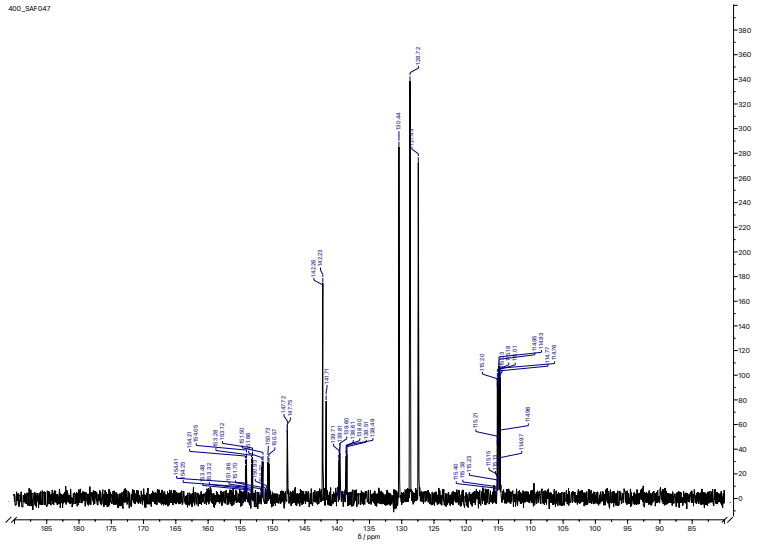

Figure S16. $^{13}C\{^{1}H\}$ NMR spectrum of $L^{7}H$ ($CDCl_3$).

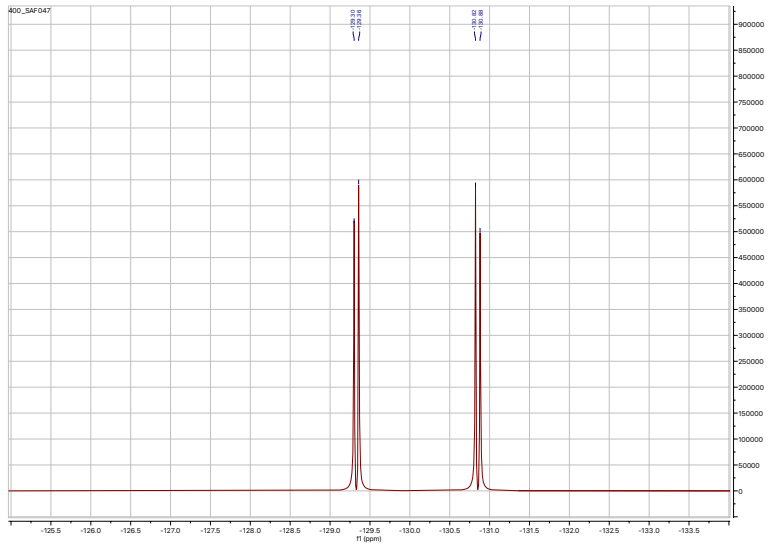

Figure S17. $^{19}F\{^{1}H\}$ NMR spectrum of $L^{7}H$ ($CDCl_3$).

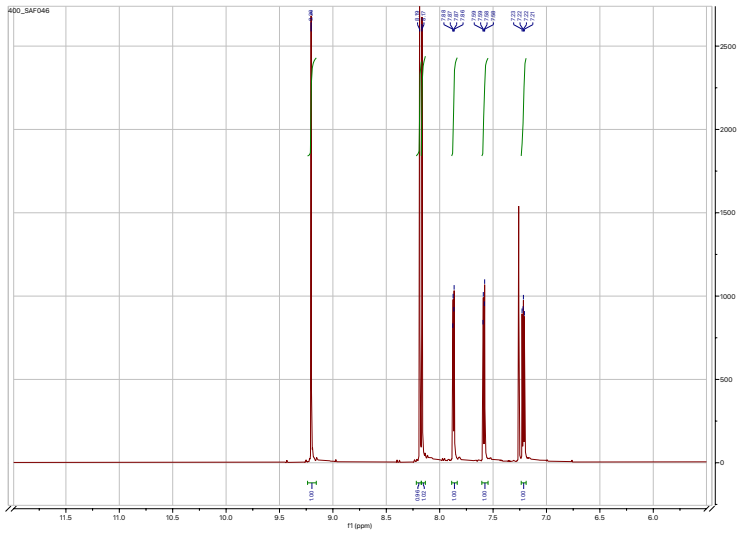

Figure S18. ^{1}H NMR spectrum of $L^{8}H$ ($CDCl_3$).

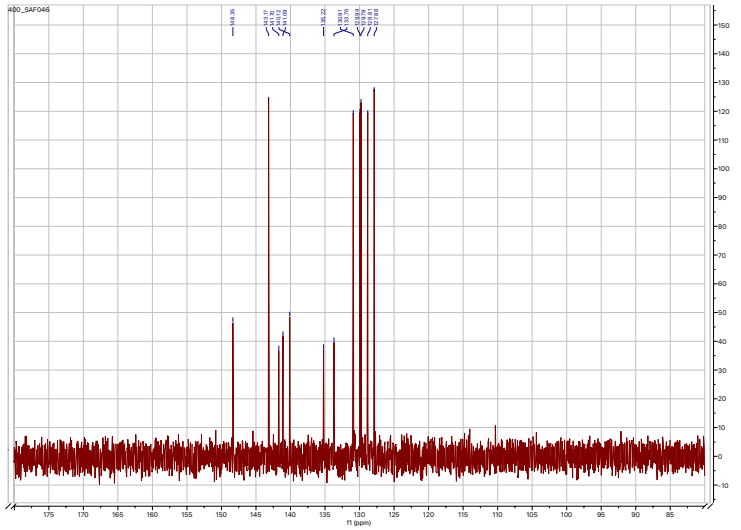

Figure S19. $^{13}C\{^{1}H\}$ NMR spectrum of $L^{8}H$ ($CDCl_3$).

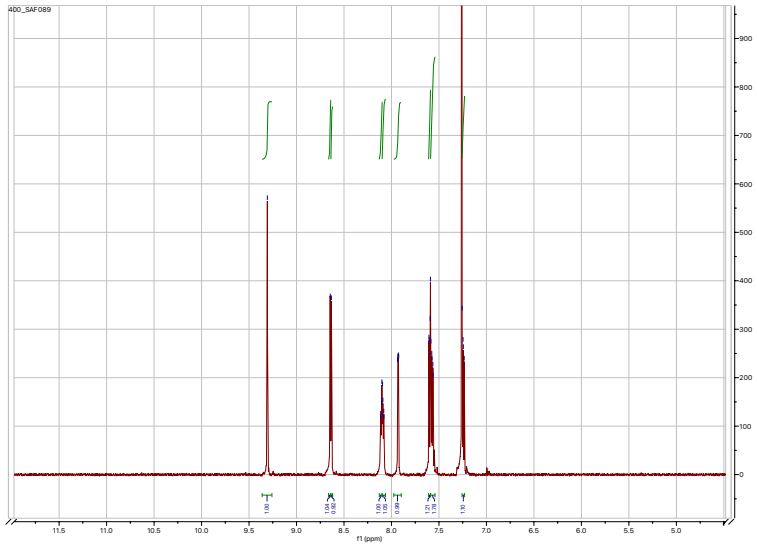

Figure S20. ^{1}H NMR spectrum of $L^{9}H$ ($CDCl_3$).

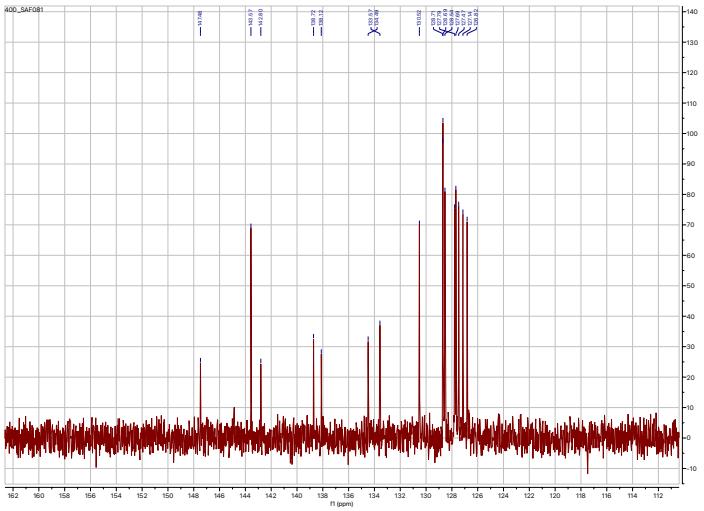

Figure S21. $^{13}C\{^{1}H\}$ NMR spectrum of $L^{9}H$ ($CDCl_3$).

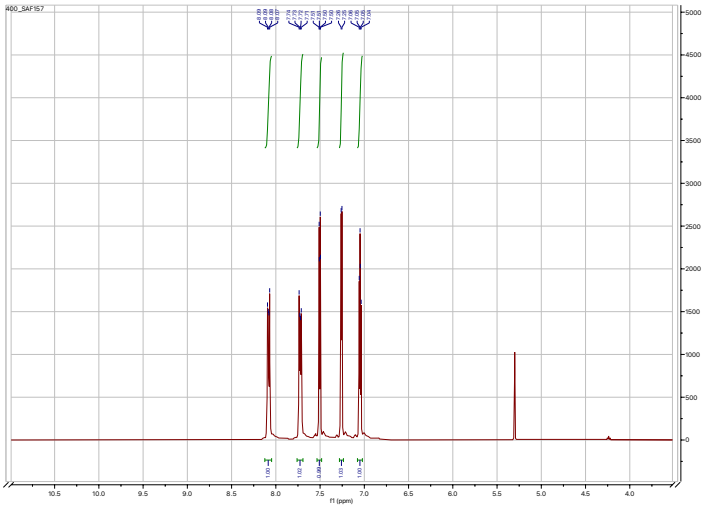

Figure S22. ^{1}H NMR spectrum of $L^{10}H$ ($CDCl_3$).

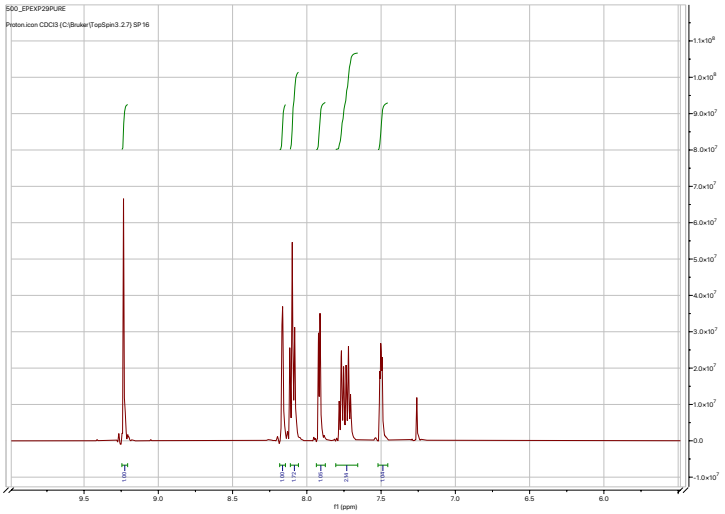

Figure S23. ^{1}H NMR spectrum of $L^{11}H$ ($CDCl_3$).

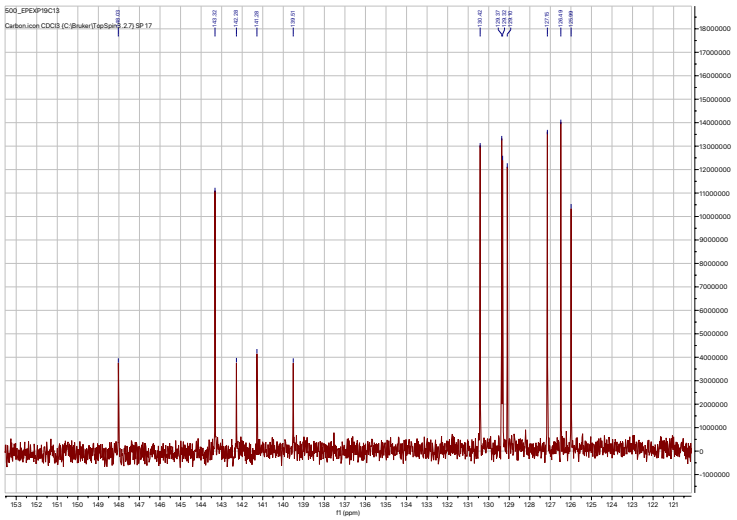

Figure S24. $^{13}C\{^{1}H\}$ NMR spectrum of $L^{11}H$ ($CDCl_3$).

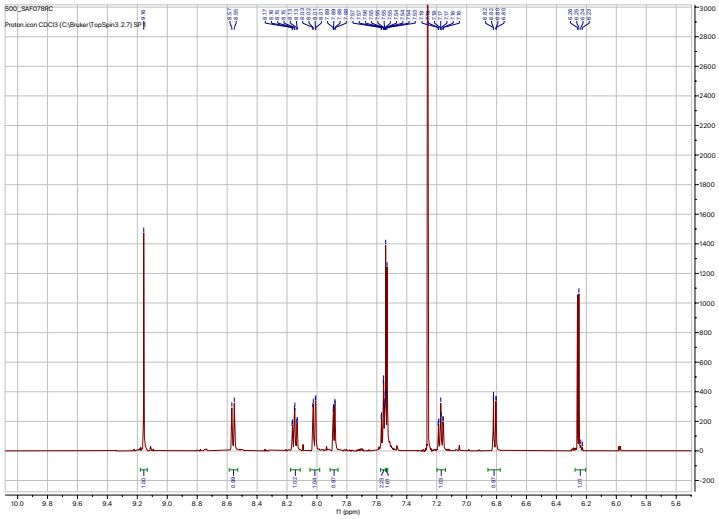

Figure S25. ^{1}H NMR spectrum of $[Ir(L^{1})_2(bipy)]PF_6$ ($CDCl_3$).

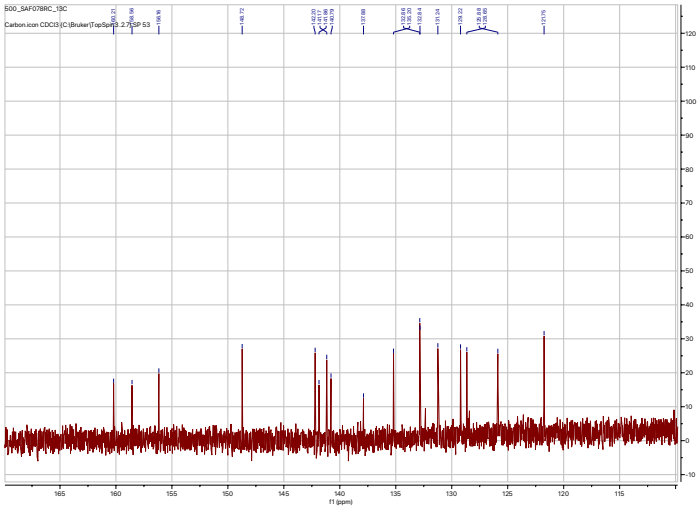

Figure S26. $^{13}C\{^{1}H\}$ NMR spectrum of $[Ir(L^{1})_2(bipy)]PF_6$ ($CDCl_3$).

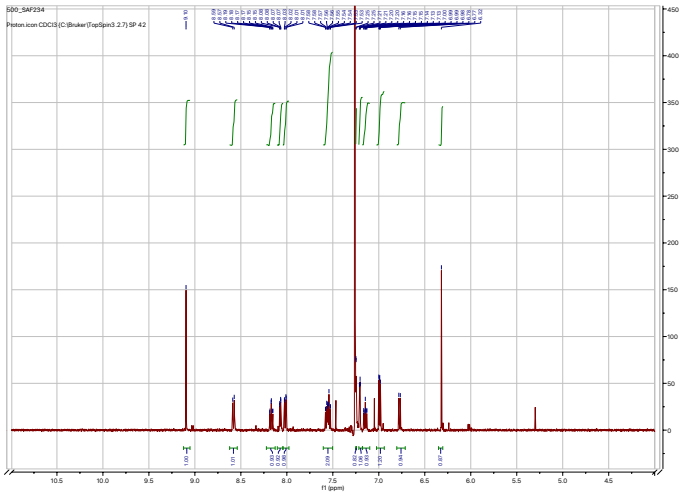

Figure S27. ^{1}H NMR spectrum of $[Ir(L^{5})_2(bipy)]PF_6$ ($CDCl_3$).

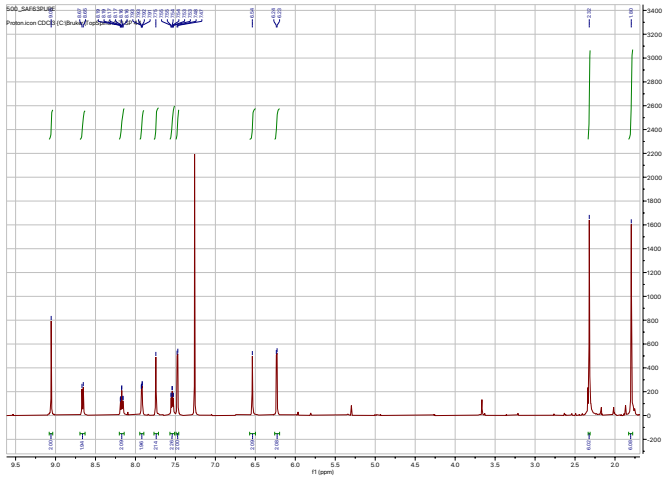

Figure S28. ^{1}H NMR spectrum of $[Ir(L^{6})_2(bipy)]PF_6$ ($CDCl_3$).

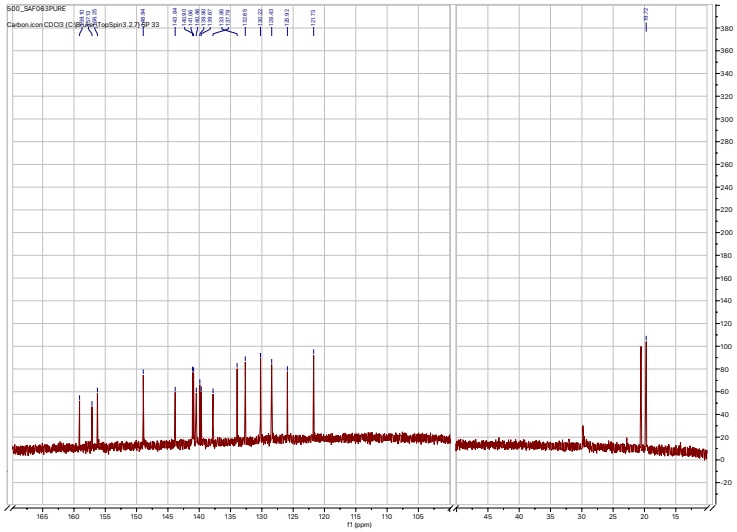

Figure S29. $^{13}C\{^{1}H\}$ NMR spectrum of $[Ir(L^{6})_2(bipy)]PF_6$ ($CDCl_3$).

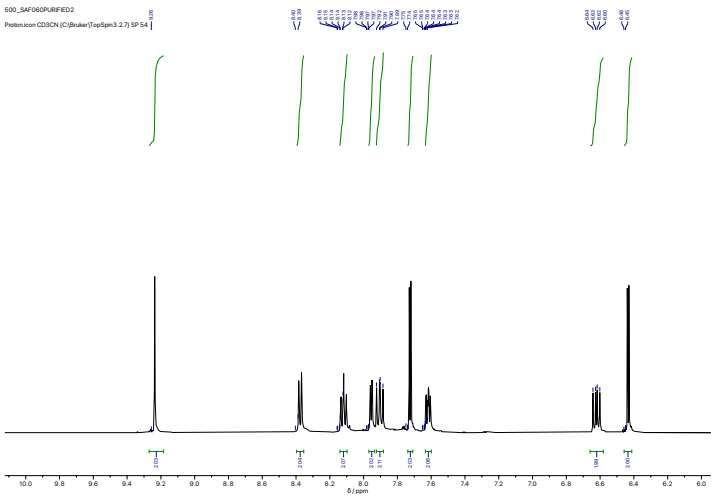

Figure S30. ^{1}H NMR spectrum of $[Ir(L^{7})_2(bipy)]PF_6$ (CD_3CN).

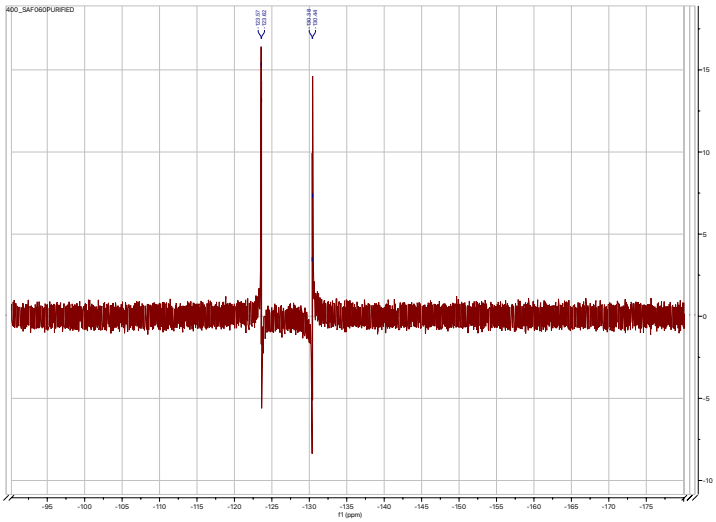

Figure S31. $^{19}F\{^{1}H\}$ NMR spectrum of $[Ir(L^{7})_2(bipy)]PF_6$ (CD_3CN).

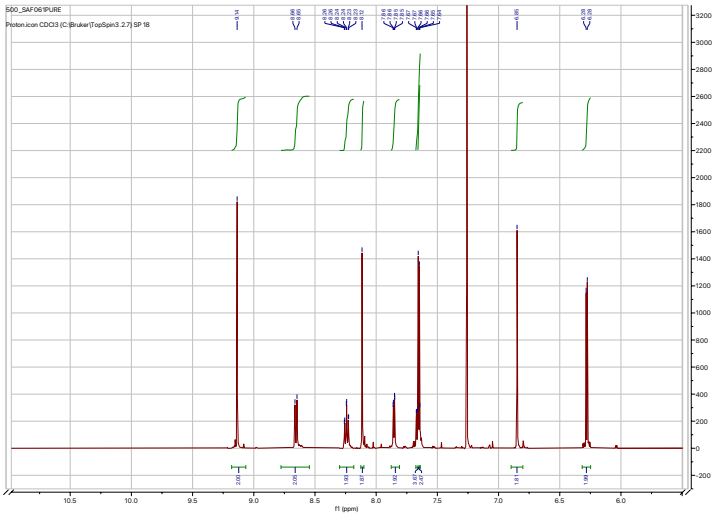

Figure S32. ^{1}H NMR spectrum of $[Ir(L^{8})_2(bipy)]PF_6$ ($CDCl_3$).

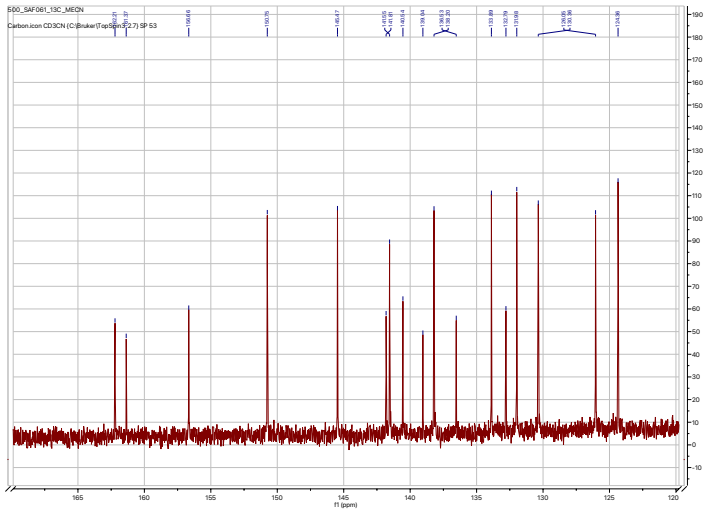

Figure S33. $^{13}C\{^{1}H\}$ NMR spectrum of $[Ir(L^{8})_2(bipy)]PF_6$ ($CDCl_3$).

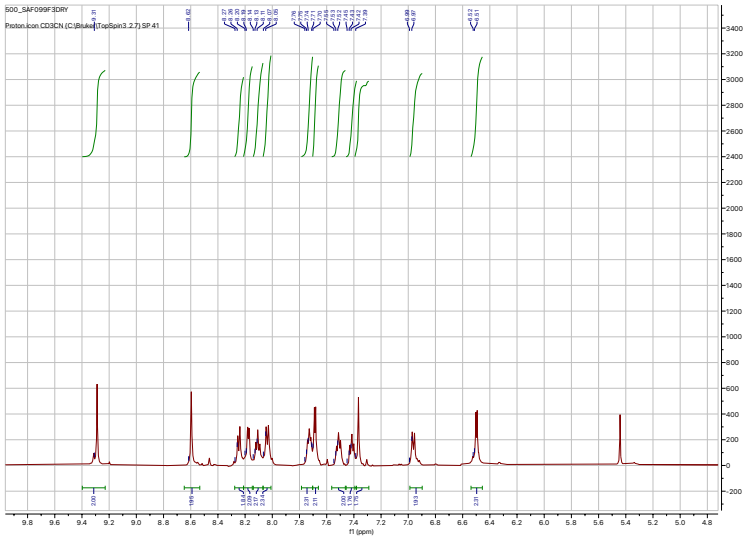

Figure S34. ^{1}H NMR spectrum of $[Ir(L^{9})_2(bipy)]PF_6$ (CD_3CN).

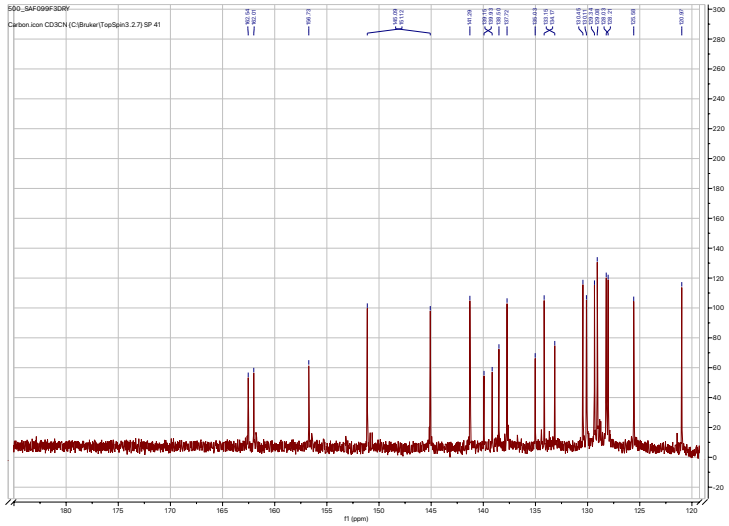

Figure S35. $^{13}C\{^{1}H\}$ NMR spectrum of $[Ir(L^{9})_2(bipy)]PF_6$ (CD_3CN).

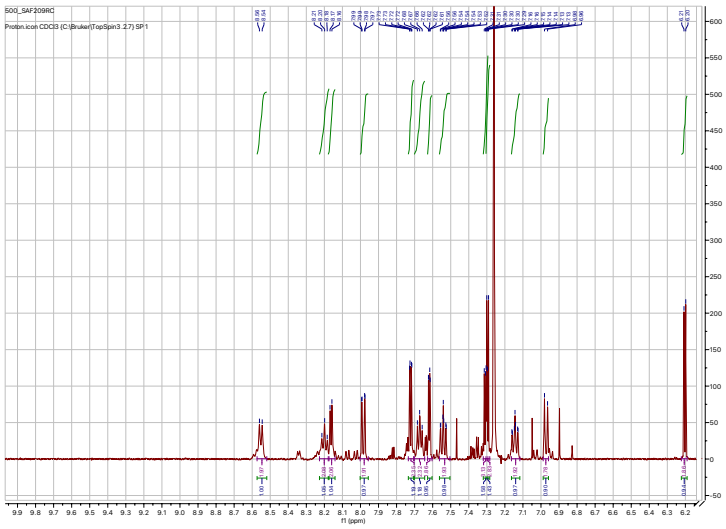

Figure S36. ^{1}H NMR spectrum of $[Ir(L^{10})_2(bipy)]PF_6$ ($CDCl_3$).

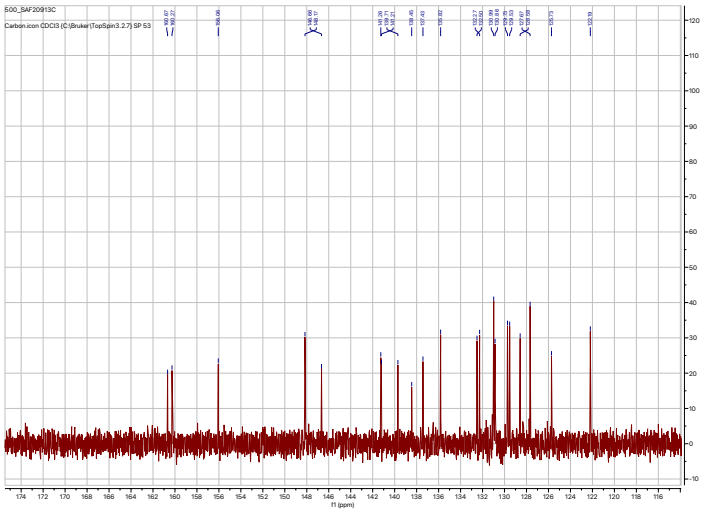

Figure S37. $^{13}C\{^{1}H\}$ NMR spectrum of $[Ir(L^{10})_2(bipy)]PF_6$ ($CDCl_3$).

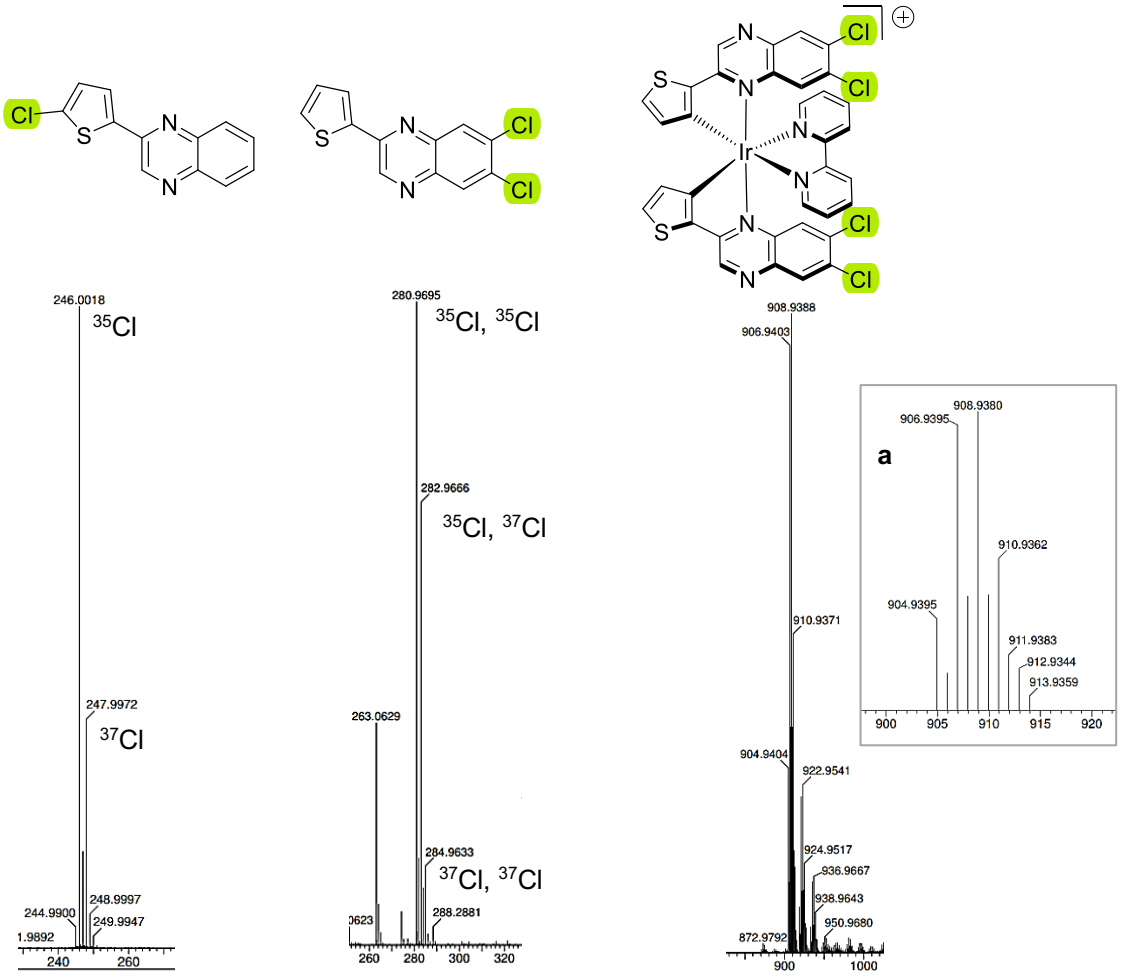

Figure S38. HRMS data for the chlorinated compounds (EI for **L^{2}H**, ESI for **L^{8}H** and [Ir(**L**^{8})$_2$(bipy)]PF$_6$) where corresponding structures are placed above. Inset:[a] magnified portion of the [Ir(**L**^{8})$_2$(bipy)]PF$_6$ spectrum showing the isotopic distribution.

Table S2. Data collection parameters for the X-ray diffraction crystal structures.

	[Ir(L^6)$_2$(bipy)]PF$_6$	**[Ir(L^8)$_2$(bipy)]PF$_6$**
Formula	$C_{38}H_{30}F_6IrN_6PS_2$	$C_{35.33}H_{20}Cl_4F_6IrN_{6.67}PS_2$
$D_{calc.}$/ g cm^{-3}	1.794	1.928
μ/mm^{-1}	3.940	3.767
Formula Weight	972.014	1081.01
Colour	red	red
Shape	block-shaped	rod-shaped
Size/mm^3	0.100×0.080×0.040	0.152×0.045×0.014
T/K	100(2)	100.15
Crystal System	triclinic	triclinic
Space Group	P-1	P-1
a/Å	11.7348(5)	14.0214(4)
b/Å	12.2893(4)	20.3990(8)
c/Å	13.6241(4)	20.6263(4)
α/°	84.601(3)	74.988(2)
β/°	75.930(3)	78.654(2)
γ/°	70.807(3)	87.905(3)
V/Å^3	1799.67(12)	5586.2(3)
Z	2	6
Z'	1	3
Wavelength/Å	0.71075	0.6889
Radiation type	Mo K$_\alpha$	Synchrotron
Θ_{min}/°	2.13	1.587
Θ_{max}/°	28.70	26.573
Measured Refl's.	41819	175892
Indep't Refl's	9285	25612
Refl's I≥2 σ(I)	5963	11600
R_{int}	0.0810	0.1388
Parameters	828	1911
Restraints	2473	5870
Largest Peak	1.1841	4.703
Deepest Hole	-0.9983	-1.953
GooF	1.0674	1.250
wR_2 (all data)	0.1020	0.4106
wR_2	0.0870	0.3724
R_1 (all data)	0.0913	0.1969
R_1	0.0430	0.1339

Detailed comment regarding structure of [Ir(L^8)$_2$(bipy)]PF_6:

For [Ir(L^8)$_2$(bipy)]PF_6, multiple crystals were attempted. The dataset used was from data collected using synchrotron radiation. There were compromises between having a large enough crystal to obtain suitable diffraction images, radiation damage to the crystal during the data collection, and having sufficient resolution to be able to determine the structure. The crystal used for data collection was not single, but most probably some sort of stacked plate with the distortion mainly about one axis. However, it did yield mostly clean diffraction spots and gave the best data from all those attempted. The data was integrated as a single component as all attempts to integrate using multiple components produced poorer results. As crystal damage was observed during the collection, attempts to compensate for this during the integration (using B-factors) were employed. A basic model was used which did improve the data quality, however it is likely that the model is an oversimplification resulting in some minor errors in the given hkl intensities. This, along with the crystal not been totally single, could explain the broadening of the F_{obs} *versus* F_{calc} graph (Figure S39). Attempts to investigate this to improve the data quality all gave worse results such that the basic settings were used in an effort to yield the basic overall structure.

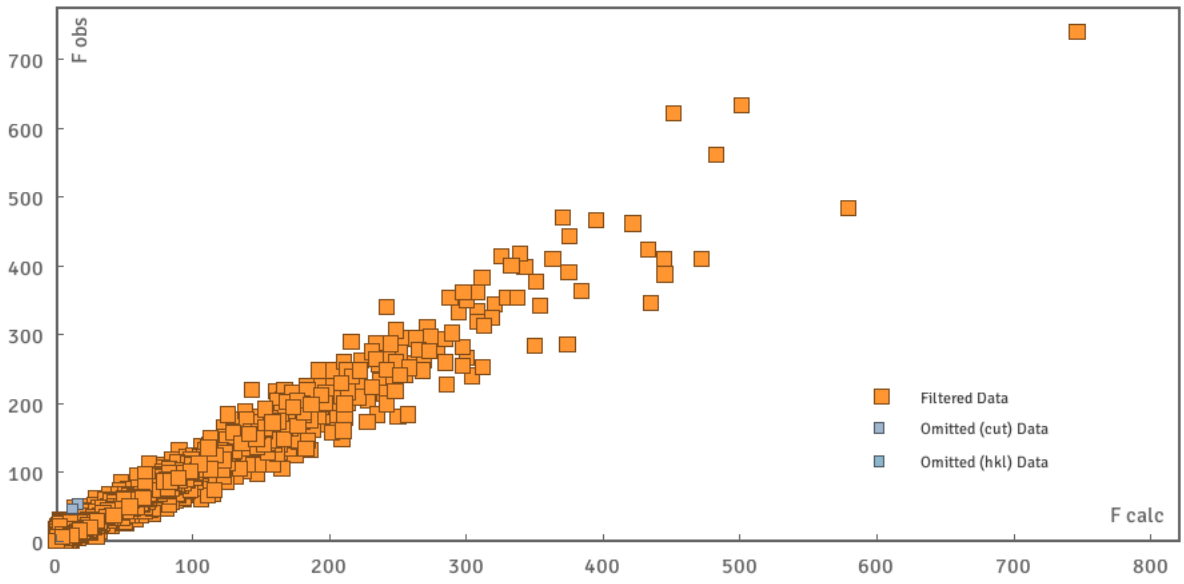

Figure S39. The F_{obs} *versus* F_{calc} plot for the data associated with [Ir(L^8)$_2$(bipy)]PF_6.

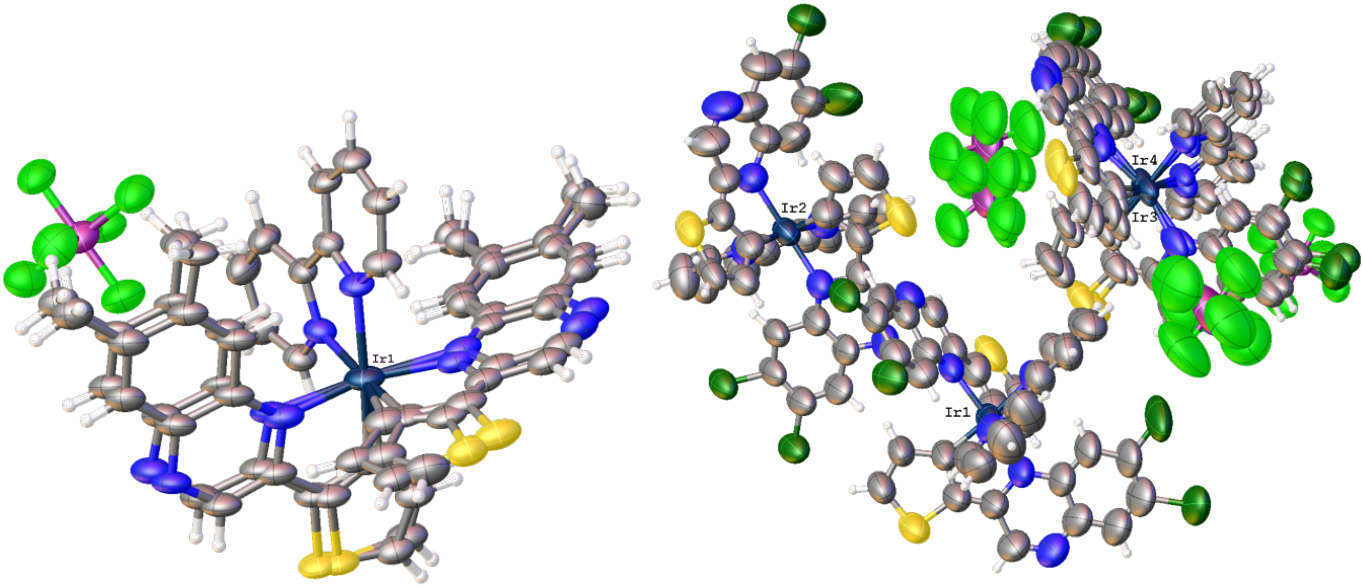

Figure S40. ORTEP representations of the structures of [Ir(**L**^{6})$_2$(bipy)]PF$_6$ (left) and [Ir(**L**^{8})$_2$(bipy)]PF$_6$ (right) obtained from single crystal X-ray diffraction.

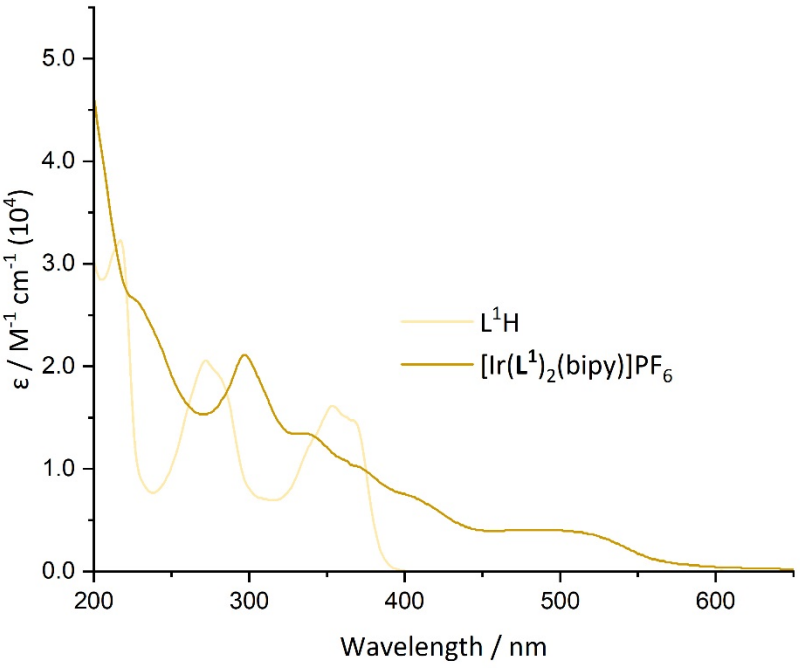

Figure S41. Room temperature (MeCN) UV-vis absorption spectra of L^{1}H and [Ir(L^1)$_2$(bipy)PF$_6$.

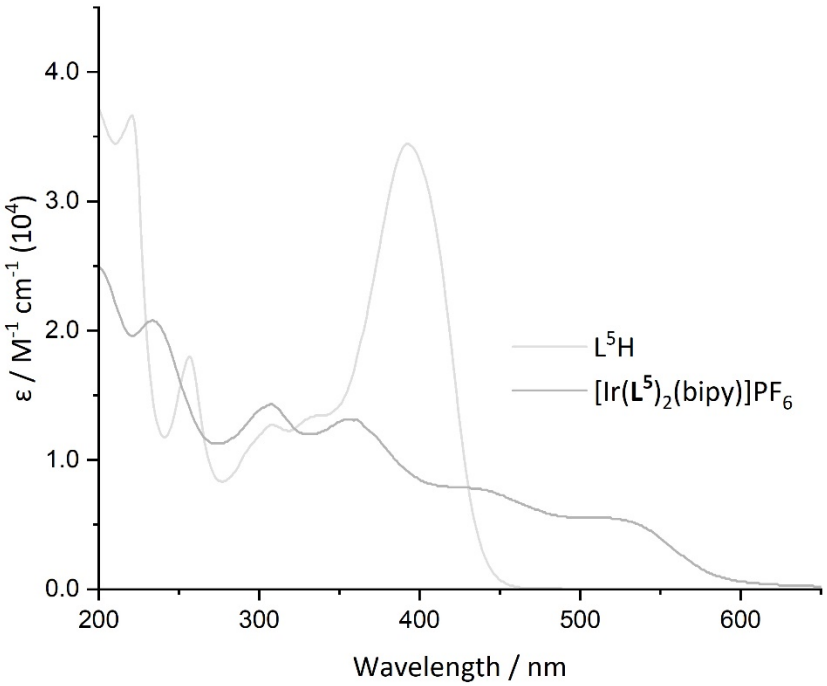

Figure S42. Room temperature (MeCN) UV-vis absorption spectra of L^5H and $[Ir(L^5)_2(bipy)PF_6$.

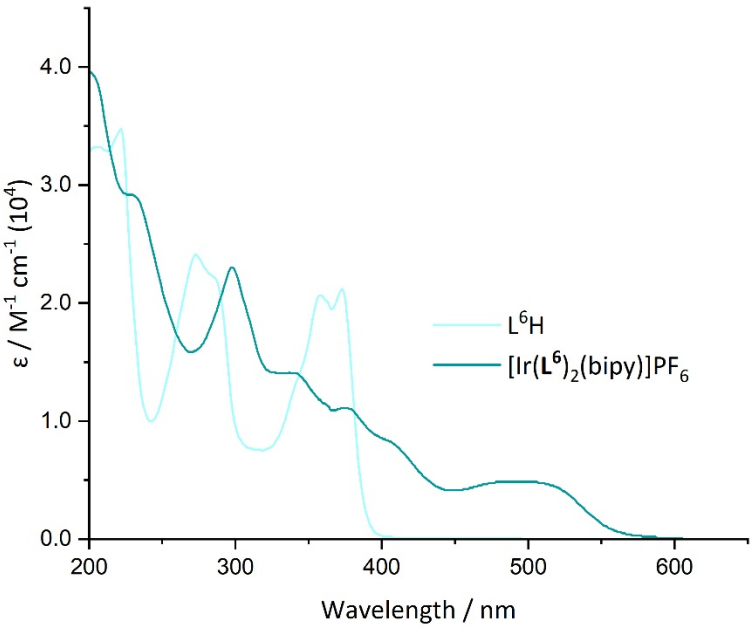

Figure S43. Room temperature (MeCN) UV-vis absorption spectra of L^6H and $[Ir(L^6)_2(bipy)PF_6$.

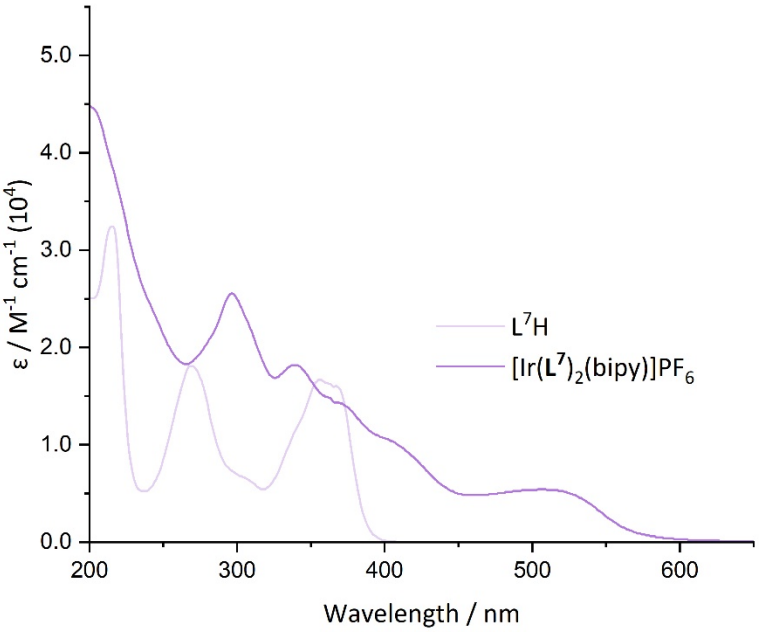

Figure S44. Room temperature (MeCN) UV-vis absorption spectra of L^7H and $[Ir(L^7)_2(bipy)PF_6$.

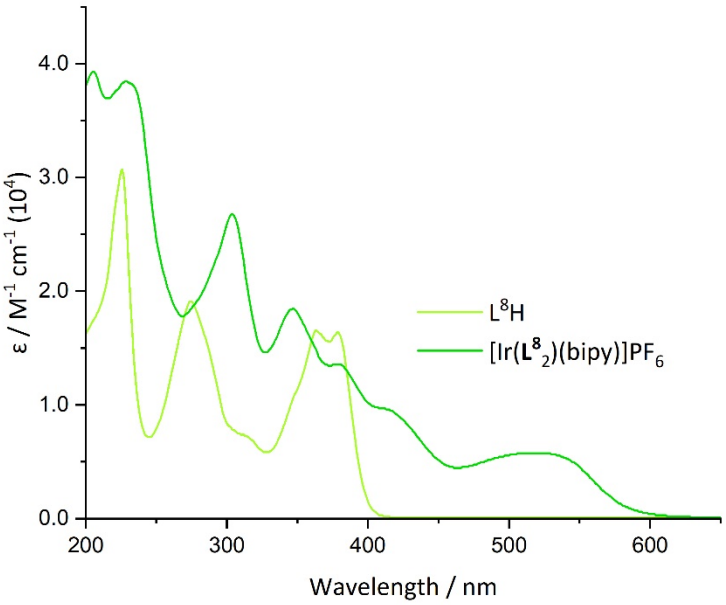

Figure S45. Room temperature (MeCN) UV-vis absorption spectra of L^8H and $[Ir(L^8)_2(bipy)PF_6$.

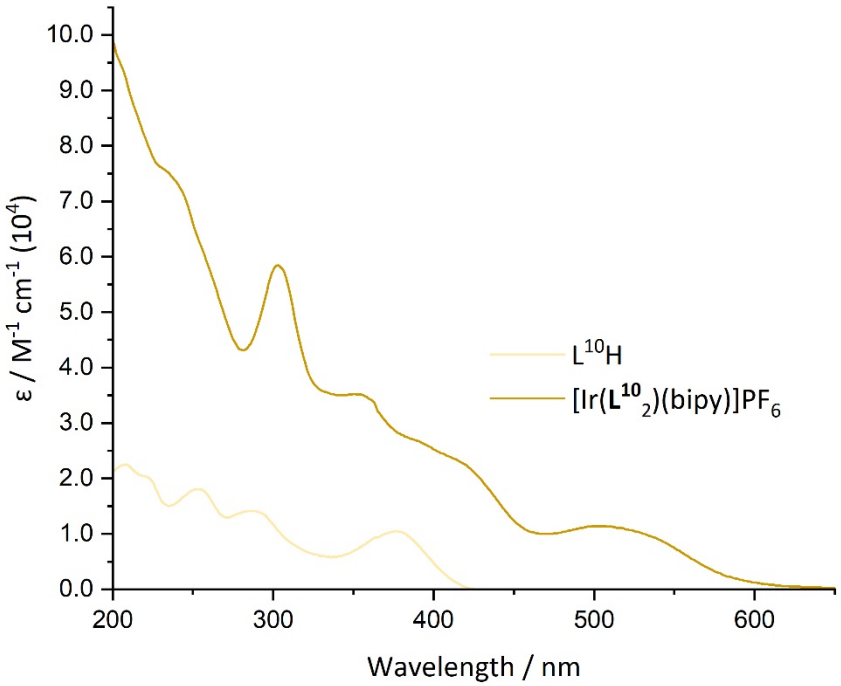

Figure S46. Room temperature (MeCN) UV-vis absorption spectra of $L^{10}H$ and $[Ir(L^{10})_2(bipy)PF_6$.

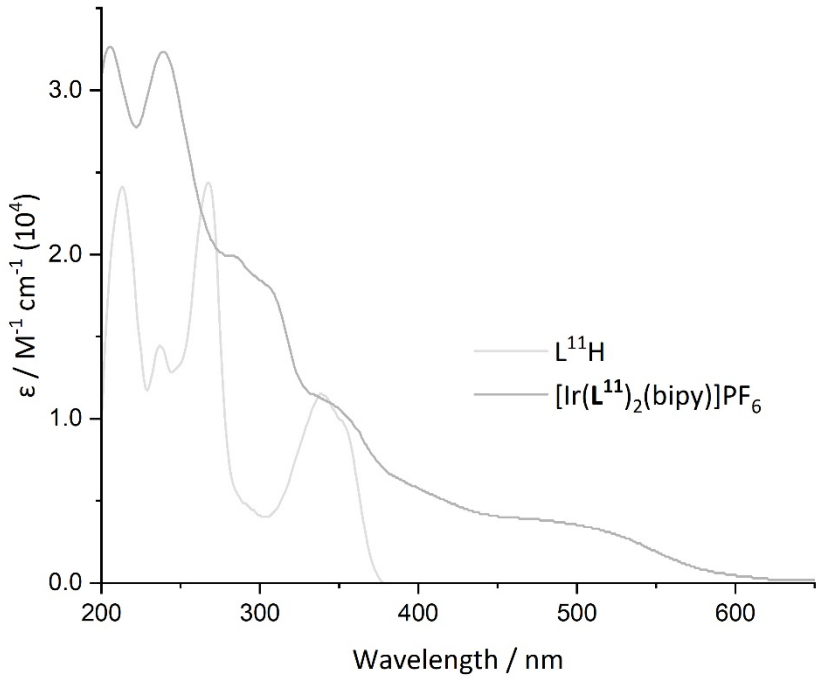

Figure S47. Room temperature (MeCN) UV-vis absorption spectra of $L^{11}H$ and $[Ir(L^{11})_2(bipy)PF_6$.

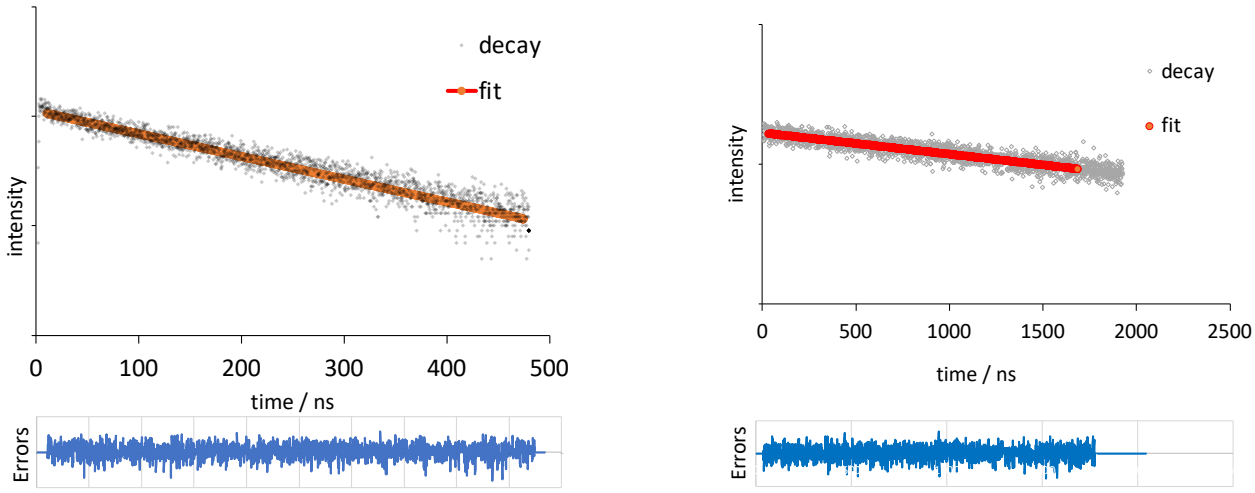

Figure S48. Examples of the fitted decay profiles (with residual errors shown beneath each decay) for $[Ir(L^8)_2(bipy)PF_6$ under aerated (left) and deoxygenated (right) conditions (MeCN, λ_{ex} = 295 nm).

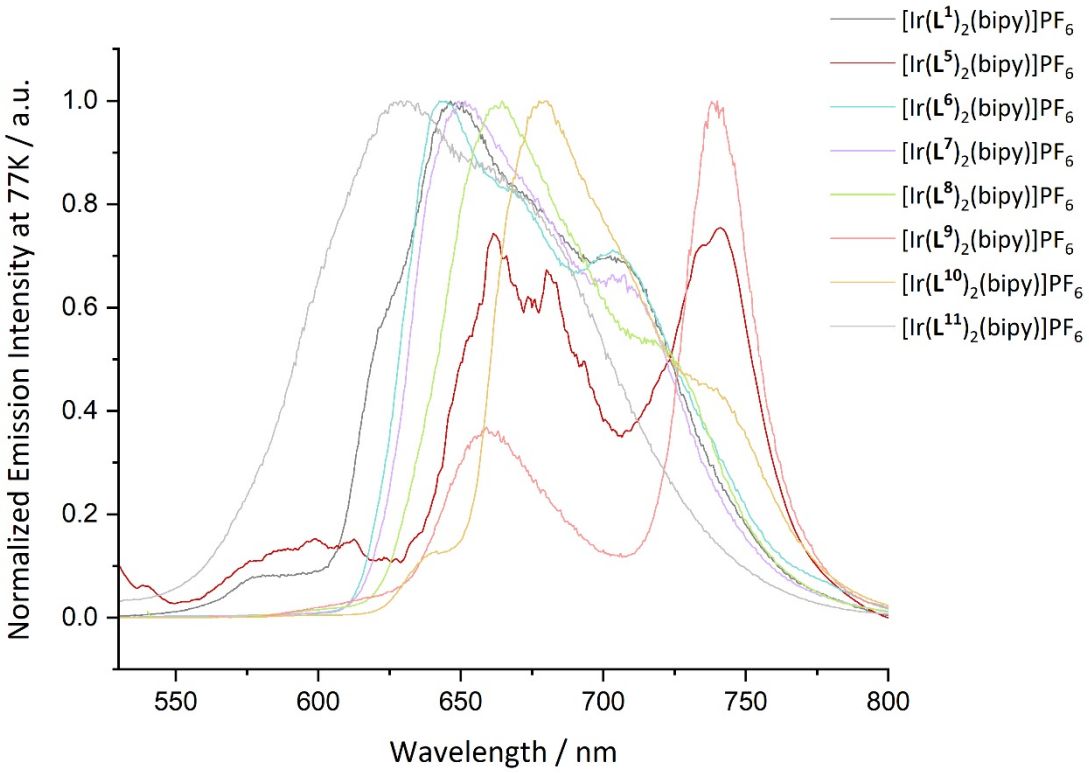

Figure S49. Comparison of the low temperature (77K, EtOH/MeOH glass) emission spectra for the complexes.

References

[1] G. Gudipudi, S. R. Sagurthi, S. Perugu, G. Achaiah and G. L. D. Krupadanam, *RSC Adv*, 2014, **4**, 56489
[2] M. Ye, Y. Wen, H. Li, Y. Fu and Q. Wang, *Tet. Lett.*, 2016, **57**, 4983
[3] K. B. Harsha and K. S. Rangappa, *RSC Adv*, 2016, **6**, 57154; K. B. Harsha, S. Rangappa, H. D. Preetham, T. R. Swaroop, M. Gilandoust, K. S. Rakesh, K. S. Rangappa, *ChemistrySelect*, 2018, **3**, 5228
[4] S. Uçar, A. Daştan, *J. Org. Chem.*, 2020, **85**, 15502
[5] F. Amaya-García, M. Caldera, A. Koren, S. Kubicek, J. Menche, M.M. Unterlass, *ChemSusChem*, 2021, **14**, 1853
[6] Y. Yang, F. Ni, W. M. Shu, A. X. Wu, *Chem. Eur. J.*, 2014, **20**, 11776